An Enhanced Solid-Shell Element Formulation with Co-Rotational Approach

Cengiz POLAT

***Abstract*—An enhanced eight node solid-shell element formulation is demonstrated. The enhanced strain method is used to alleviate the locking problems. A co-rotational formulation is adopted in the formulation, thus geometric nonlinearity is taken into account by the rotation of the local coordinate system. Several benchmark problems are studied to demonstrate the efficiency of the element.**

***Index Terms*— Co-rotational formulation, solid-shell element, the enhanced strain method.**

I. INTRODUCTION

In the linear analysis, the displacements and strains developed in the structure are small. That is, the geometry of the structure assumed remains unchanged during the loading process and linear strain approximations can be used. However, the geometry of the structure changes continuously during the loading process, and this fact is taken into account in the geometrically nonlinear analysis [1, 2]. Mainly, three Lagrangian kinematic descriptions are in present use for finite element analysis of geometrically nonlinear structures: Total Lagrangian (TL), Updated Lagrangian (UL) and Co-Rotational (CR) formulation [3]. The pioneers of the co-rotational approach can be said as Wempner [4], Argyris et al. [5], Belytschko and Glaum [6], Crisfield and Moita [7] and Moita and Crisfield [8]. The attractiveness of the CR formulation resides in the fact that it can be applied to simplify the Lagrangian formulations for large-displacement and small-strain problems without significant loss of accuracy [9]. In this formulation the rigid-body motion is eliminated and only element deformation is considered to obtain the internal forces and the tangent stiffness matrix.

Many researchers [10-19] are interested in solid-shell elements which are widely used to analyze shell like structures. These elements possess no rotational degrees-of-freedom. Thus, the complication on handling finite rotational increments can be avoided. However, similar to the degenerated shell elements these elements also suffer from some kind of locking effects. Various methods have been suggested to overcome these locking effects. The earliest techniques are Uniform Reduced Integration (URI) [20] and Selective Reduced Integration (SRI) [21, 22]. However, URI procedure generally leads to spurious zero energy modes, despite the fact that for some cases a correct solution is obtained. In addition, SRI procedure exhibits similar problems but usually on a smaller range.

Revised Version Manuscript Received on March 14, 2017.

Dr. Cengiz POLAT, Firat University, Technical Vocational School, Elazig, Turkey. E-mail: cpolat@firat.edu.tr

Another two distinct approaches are the Assumed Natural Strain (ANS) [23, 24] and the Enhanced Assumed Strain (EAS) [25-27] which are successfully implemented in various finite elements to alleviate locking effects.

The objective of this paper is to demonstrate the nearly locking free formulation of an 8-node solid-shell element based on the co-rotational description of motion. Firstly, the geometry and the strain-displacement relations of the displacement based 8-node solid-shell element are presented. Low order elements based on standard displacement interpolation are usually accompanied by locking phenomena. To alleviate locking problems of the element, an enhanced strain method is used. The enhanced strain method is based on the enhancing of the displacement-dependent strain field by an extra assumed strain field, and it is assumed that the stress and the enhanced assumed strain fields are orthogonal, which results in an elimination of the stress field from the finite element equations. Secondly, a co-rotational formulation based on the study of Crisfield and Moita [7], Moita and Crisfield [8], Felippa and Haugen [3] is given. A local coordinate system is attached to the element and a rotation matrix which defines the rotation of this local coordinate system according to the global coordinate system, is obtained using the polar decomposition theorem. Thus, the geometric non-linearity is incorporated by the rotation of the local coordinate system. Lastly, several benchmark problems are examined by a computer program which is written by the author in MATLAB code.

II. ELEMENT FORMULATION

A. Geometry of the Solid Shell Element

The coordinates of a typical point in the eight node solid-shell element (Fig. 1.) can be written as

$$\mathbf{x}=\sum_{k=1}^{4} N_k\left(\frac{1+\zeta}{2}\mathbf{x}_k^t+\frac{1-\zeta}{2}\mathbf{x}_k^b\right) \qquad (1)$$

where $N_k = N_k(\xi,\eta)$ are the two-dimensional isoparametric shape functions, $\mathbf{x}=[x,y,z]^T$ are the position vectors; ξ, η and ζ are curvilinear coordinates. Here ξ, η and ζ are assumed to vary from -1 and +1.

The displacement field $\mathbf{u}=[u,v,w]^T$ in the shell element can be approximated by

Published By:
Blue Eyes Intelligence Engineering
& Sciences Publication Pvt. Ltd.

$$\mathbf{u} = \sum_{k=1}^{4} N_k \left(\frac{1+\zeta}{2} \mathbf{u}_k^t + \frac{1-\zeta}{2} \mathbf{u}_k^b \right) \tag{2}$$

where $\mathbf{u}_k = [u_k, v_k, w_k]^T$ represents the displacement vector of node k [1,2].

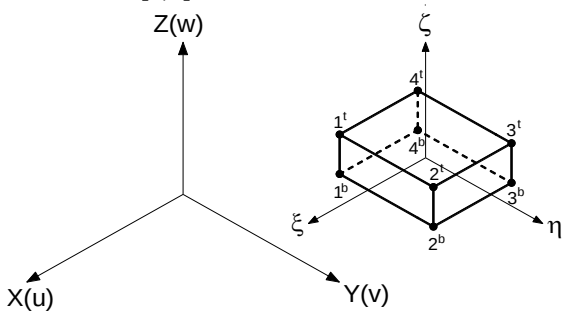

Figure 1. Geometry of the Eight Node Solid-Shell Element.

B. Strain–Displacement Relationships

The components of the displacement-based strain tensor $\boldsymbol{\varepsilon}^u$ in the natural set of coordinates (ξ, η, ζ) can be given as

$$\boldsymbol{\varepsilon}^u = [\varepsilon^u_{\xi\xi} \quad \varepsilon^u_{\eta\eta} \quad \varepsilon^u_{\zeta\zeta} \quad \varepsilon^u_{\xi\eta} \quad \varepsilon^u_{\xi\zeta} \quad \varepsilon^u_{\eta\zeta}]^T \tag{3}$$

or

$$\boldsymbol{\varepsilon}^u = \mathbf{B}^u \mathbf{u}, \qquad \mathbf{u} = [\mathbf{u}_1 \ . \ . \ . \ \mathbf{u}_k]^T \qquad k = 1,...n \tag{4}$$

where $\mathbf{B}^u$ is the conventional strain-displacement matrix and $\mathbf{u}$ is the nodal displacement vector. The natural strain components defined in Eq. (3) can be determined [19] by using the displacement vector $\mathbf{u}$ and the covariant base vectors $\mathbf{g}_i$ as

$$\varepsilon^u_{\xi_i \xi_j} = \frac{1}{2} \left(\frac{\partial \mathbf{u}}{\partial \xi_i} \mathbf{g}_j + \frac{\partial \mathbf{u}}{\partial \xi_j} \mathbf{g}_i \right) \quad (i, j = 1, 2, 3; \ \xi_1 = \xi, \ \xi_2 = \eta, \ \xi_3 = \zeta \tag{5}$$

and

$$\mathbf{g}_i = \frac{\partial \mathbf{x}}{\partial \xi_i} \tag{6}$$

where $\mathbf{x}$ is the position vector.

The previously described strain field is related to the natural set of coordinates. Therefore, it is necessary to obtain the local physical strains from the natural strain components. An algorithm suggested by Valente [28] is used for the transformation of the strains. It consists of the following five steps:

a) $\mathbf{r}^3 = \left[\frac{\partial x}{\partial \xi} \ \frac{\partial y}{\partial \xi} \ \frac{\partial z}{\partial \xi} \right]^T \times \left[\frac{\partial x}{\partial \eta} \ \frac{\partial y}{\partial \eta} \ \frac{\partial z}{\partial \eta} \right]^T$

b) $\mathbf{r}^3 = \frac{\mathbf{r}^3}{\|\mathbf{r}^3\|}$

c) $\mathbf{r}^1 = \left[\frac{\partial x}{\partial \xi} \ \frac{\partial y}{\partial \xi} \ \frac{\partial z}{\partial \xi} \right]^T$

d) $\mathbf{r}^1 = \frac{\mathbf{r}^1}{\|\mathbf{r}^1\|}$

e) $\mathbf{r}^2 = \mathbf{r}^3 \times \mathbf{r}^1$

Then, the components of director cosines matrix $\hat{\mathbf{T}}$ is

$$\hat{\mathbf{T}} = \left[\mathbf{r}^1 \quad \mathbf{r}^2 \quad \mathbf{r}^3 \right]^T (\mathbf{J})^{-1} \tag{7}$$

in which $\mathbf{J}$ is the conventional Jacobian matrix given by

$$\mathbf{J} = \begin{bmatrix} \frac{\partial x}{\partial \xi} & \frac{\partial y}{\partial \xi} & \frac{\partial z}{\partial \xi} \\ \frac{\partial x}{\partial \eta} & \frac{\partial y}{\partial \eta} & \frac{\partial z}{\partial \eta} \\ \frac{\partial x}{\partial \zeta} & \frac{\partial y}{\partial \zeta} & \frac{\partial z}{\partial \zeta} \end{bmatrix} \tag{8}$$

The natural coordinate and the local coordinate system can be related by the second-order transformation tensor $\bar{\mathbf{T}}$

$$\bar{\mathbf{T}} = \begin{bmatrix} \hat{T}_{11}\hat{T}_{11} & \hat{T}_{12}\hat{T}_{12} & \hat{T}_{13}\hat{T}_{13} & \hat{T}_{11}\hat{T}_{12} & \hat{T}_{11}\hat{T}_{13} & \hat{T}_{12}\hat{T}_{13} \\ \hat{T}_{21}\hat{T}_{21} & \hat{T}_{22}\hat{T}_{22} & \hat{T}_{23}\hat{T}_{23} & \hat{T}_{21}\hat{T}_{22} & \hat{T}_{21}\hat{T}_{23} & \hat{T}_{22}\hat{T}_{23} \\ \hat{T}_{31}\hat{T}_{31} & \hat{T}_{32}\hat{T}_{32} & \hat{T}_{33}\hat{T}_{33} & \hat{T}_{31}\hat{T}_{32} & \hat{T}_{31}\hat{T}_{33} & \hat{T}_{32}\hat{T}_{33} \\ 2\hat{T}_{11}\hat{T}_{21} & 2\hat{T}_{12}\hat{T}_{22} & 2\hat{T}_{13}\hat{T}_{23} & \hat{T}_{11}\hat{T}_{22}+\hat{T}_{12}\hat{T}_{21} & \hat{T}_{11}\hat{T}_{23}+\hat{T}_{21}\hat{T}_{13} & \hat{T}_{12}\hat{T}_{23}+\hat{T}_{22}\hat{T}_{13} \\ 2\hat{T}_{11}\hat{T}_{31} & 2\hat{T}_{12}\hat{T}_{32} & 2\hat{T}_{13}\hat{T}_{33} & \hat{T}_{11}\hat{T}_{32}+\hat{T}_{12}\hat{T}_{31} & \hat{T}_{11}\hat{T}_{33}+\hat{T}_{31}\hat{T}_{13} & \hat{T}_{12}\hat{T}_{33}+\hat{T}_{32}\hat{T}_{13} \\ 2\hat{T}_{21}\hat{T}_{31} & 2\hat{T}_{22}\hat{T}_{32} & 2\hat{T}_{23}\hat{T}_{33} & \hat{T}_{21}\hat{T}_{32}+\hat{T}_{22}\hat{T}_{31} & \hat{T}_{21}\hat{T}_{33}+\hat{T}_{31}\hat{T}_{23} & \hat{T}_{22}\hat{T}_{33}+\hat{T}_{32}\hat{T}_{23} \end{bmatrix} \tag{9}$$

When you submit your final version, after your paper has been accepted, prepare it in two-column format, including figures and tables.

C. Locking Treatments

In the pure displacement-based finite element formulation of shells, employing the full quadrature rules leads to locking effects related to transverse shear strain energy values. These formulations give unacceptable results especially thickness values become smaller. To resolve the locking problems without reducing the quadrature rules, an enhanced strain method proposed by Sousa et al. is used [29]. The displacement-based strain field can be improved using the enhanced strain method as following

$$\boldsymbol{\varepsilon} = \boldsymbol{\varepsilon}^u + \boldsymbol{\varepsilon}^\alpha \tag{10}$$

where $\boldsymbol{\varepsilon}$ is the improved strain field, $\boldsymbol{\varepsilon}^u$ is the displacement-based strain tensor and $\boldsymbol{\varepsilon}^\alpha$ is the additive enhanced strain field. The additive enhanced strain field can be rewritten as

$$\boldsymbol{\varepsilon}^{\alpha} = \mathbf{B}^{\alpha}\boldsymbol{\alpha} \qquad \boldsymbol{\alpha} = \begin{bmatrix}\alpha_1 & \alpha_2 & \cdots & \alpha_{12}\end{bmatrix}^{\mathrm{T}} \tag{11}$$

where $\mathbf{B}^{\alpha}$ and is the enhanced strain field interpolation matrix, $\boldsymbol{\alpha}$ is the enhanced variables field. The enhanced strain field interpolation matrix is given by

$$\mathbf{B}^{\alpha} = \begin{bmatrix}
\frac{\partial N_\alpha}{\partial \xi} & 0 & 0 & 0 & 0 & 0 & 0 & 0 & 0 & \frac{\partial^2 N_\alpha}{\partial \xi \partial \eta} & \frac{\partial^2 N_\alpha}{\partial \xi \partial \zeta} & \frac{\partial^2 N_\alpha}{\partial \eta \partial \zeta} \\
0 & \frac{\partial N_\alpha}{\partial \eta} & 0 & 0 & 0 & 0 & 0 & 0 & 0 & \frac{\partial^2 N_\alpha}{\partial \xi \partial \eta} & \frac{\partial^2 N_\alpha}{\partial \xi \partial \zeta} & \frac{\partial^2 N_\alpha}{\partial \eta \partial \zeta} \\
0 & 0 & \frac{\partial N_\alpha}{\partial \zeta} & 0 & 0 & 0 & 0 & 0 & 0 & \frac{\partial^2 N_\alpha}{\partial \xi \partial \eta} & \frac{\partial^2 N_\alpha}{\partial \xi \partial \zeta} & \frac{\partial^2 N_\alpha}{\partial \eta \partial \zeta} \\
0 & 0 & 0 & \frac{\partial N_\alpha}{\partial \xi} & \frac{\partial N_\alpha}{\partial \eta} & 0 & 0 & 0 & 0 & 0 & 0 & 0 \\
0 & 0 & 0 & 0 & 0 & \frac{\partial N_\alpha}{\partial \xi} & \frac{\partial N_\alpha}{\partial \zeta} & 0 & 0 & 0 & 0 & 0 \\
0 & 0 & 0 & 0 & 0 & 0 & 0 & \frac{\partial N_\alpha}{\partial \eta} & \frac{\partial N_\alpha}{\partial \zeta} & 0 & 0 & 0
\end{bmatrix} \tag{12}$$

where N_{α} is the bubble function defined by

$$\mathrm{N}_{\alpha} = \frac{1}{2}(1-\xi^2)(1-\eta^2)(1-\zeta^2) \tag{13}$$

The natural coordinate and the local coordinate system can be related by the second-order transformation tensor. Thus, the strain components in the local frame $\bar{\boldsymbol{\varepsilon}}$

$$\bar{\boldsymbol{\varepsilon}}^{u} = [\bar{\varepsilon}^{u}_{xx} \quad \bar{\varepsilon}^{u}_{yy} \quad \bar{\varepsilon}^{u}_{zz} \quad \bar{\varepsilon}^{u}_{xy} \quad \bar{\varepsilon}^{u}_{xz} \quad \bar{\varepsilon}^{u}_{yz}]^{\mathrm{T}} \tag{14}$$

$$\bar{\boldsymbol{\varepsilon}}^{u} = \mathbf{T}_0\boldsymbol{\varepsilon}^{u} = \bar{\mathbf{B}}^{u}\mathbf{u} \tag{15}$$

$$\bar{\boldsymbol{\varepsilon}}^{\alpha} = \frac{\det \mathbf{J}_0}{\det \mathbf{J}}\mathbf{T}_0\boldsymbol{\varepsilon}^{\alpha} = \bar{\mathbf{B}}^{\alpha}\boldsymbol{\alpha} \tag{16}$$

where $\mathbf{J}$ is the Jacobian matrix, and $\overline{\mathbf{T}}_0$ is evaluated at the element center.

D. Co-Rotational Formulation

The initial local system coordinates $\mathbf{X}^{\mathrm{k}}_{\mathrm{L}}$ of node k can be given as

$$\mathbf{X}^{\mathrm{k}}_{\mathrm{L}} = \mathbf{X}^{\mathrm{k}} - \mathbf{X}^{1} \tag{17}$$

It is considered that the initial coordinates in the local and global systems are the same.
To obtain the local axes within the nonlinear process, it is necessary to determine the rotation matrix $\mathbf{R}$. The incremental global deformation gradient $\mathbf{F}$ computed at the center of the element can be written as

$$\mathbf{F} = \mathbf{R}\mathbf{U} \tag{18}$$

where $\mathbf{U}$ is right stretch tensor. The rotation matrix can be evaluated from the well-known the polar decomposition theorem, mostly with the determination of the eigenvalues of the right Cauchy-Green tensor.

Thus, the rotation matrix $\mathbf{R}$ is

$$\mathbf{R} = \begin{bmatrix}\mathbf{e}_1 & \mathbf{e}_2 & \mathbf{e}_3\end{bmatrix} \tag{19}$$

where $\mathbf{e}_1$, $\mathbf{e}_2$ and $\mathbf{e}_3$ are the local rotated unit vectors. The relationship between the local and global current position vectors of node k is explicitly given by

$$\mathbf{x}^{k}_{L} = \mathbf{X}^{k} + \mathbf{u}^{k}_{L} = \begin{Bmatrix}X_L \\ Y_L \\ Z_L\end{Bmatrix}^{k} + \begin{Bmatrix}u_L \\ v_L \\ w_L\end{Bmatrix}^{k} = \mathbf{R}^{T}(\mathbf{x}^{k}_{G} - \mathbf{x}^{1}_{G}) = \mathbf{R}^{T}\mathbf{x}^{k1}_{G} \tag{20}$$

where $\mathbf{x}^{\mathrm{k}}_{\mathrm{L}}$ and $\mathbf{x}^{\mathrm{k}}_{\mathrm{G}}$ are the current coordinates for the local and global position vectors for the node k, respectively.
The differentiation of Eq. (20) gives the relationship between the variation of the local displacements and the variation of the global displacements,

$$\delta\mathbf{u}^{\mathrm{k}}_{\mathrm{L}} = \mathbf{R}^{\mathrm{T}}\delta\mathbf{u}^{\mathrm{k}}_{\mathrm{G}} + \delta\mathbf{R}^{\mathrm{T}}\mathbf{x}^{\mathrm{k1}}_{\mathrm{G}} \tag{21}$$

We can rewrite Eq. (21) using a skew-symmetric matrix $\mathbf{S}$

$$\mathbf{S}(\mathbf{x}^{\mathrm{k1}}_{\mathrm{G}}) = \begin{bmatrix} 0 & -\mathrm{z}^{\mathrm{k1}}_{\mathrm{G}} & \mathrm{y}^{\mathrm{k1}}_{\mathrm{G}} \\ \mathrm{z}^{\mathrm{k1}}_{\mathrm{G}} & 0 & -\mathrm{x}^{\mathrm{k1}}_{\mathrm{G}} \\ -\mathrm{y}^{\mathrm{k1}}_{\mathrm{G}} & -\mathrm{x}^{\mathrm{k1}}_{\mathrm{G}} & 0 \end{bmatrix} \tag{22}$$

$$\delta\mathbf{u}^{\mathrm{k}}_{\mathrm{L}} = \mathbf{R}^{\mathrm{T}}\delta\mathbf{u}^{\mathrm{k}}_{\mathrm{G}} + \mathbf{R}^{\mathrm{T}}\mathbf{S}(\mathbf{x}^{\mathrm{k1}}_{\mathrm{G}})\delta\boldsymbol{\theta} \tag{23}$$

we can rewrite Eq. (23) at the element level as

$$\delta\mathbf{u}_{\mathrm{L}} = \left[\mathrm{diag}\,\mathbf{R}^{\mathrm{T}}\right]\delta\mathbf{u}_{\mathrm{G}} + \left[\mathrm{col}\,(\mathbf{R}^{\mathrm{T}}\mathbf{S}(\mathbf{x}^{\mathrm{k1}}_{\mathrm{G}}))\right]\delta\boldsymbol{\theta} \tag{24}$$

where $\delta\boldsymbol{\theta}$ is a pseudo-vector. To find an expression for the pseudo-vector $\delta\boldsymbol{\theta}$, we can write a spin vector $\boldsymbol{\Omega}$ using local quantities

$$\boldsymbol{\Omega} = \begin{bmatrix} \frac{\partial \mathrm{u}_{\mathrm{L}}}{\partial \mathrm{Y}_{\mathrm{L}}} - \frac{\partial \mathrm{v}_{\mathrm{L}}}{\partial \mathrm{X}_{\mathrm{L}}} \\ \frac{\partial \mathrm{u}_{\mathrm{L}}}{\partial \mathrm{Z}_{\mathrm{L}}} - \frac{\partial \mathrm{w}_{\mathrm{L}}}{\partial \mathrm{X}_{\mathrm{L}}} \\ \frac{\partial \mathrm{v}_{\mathrm{L}}}{\partial \mathrm{Z}_{\mathrm{L}}} - \frac{\partial \mathrm{w}_{\mathrm{L}}}{\partial \mathrm{Y}_{\mathrm{L}}} \end{bmatrix} = \mathbf{A}^{\mathrm{T}}_{\mathrm{L}}\mathbf{u}_{\mathrm{L}} = 0 \tag{25}$$

where $\mathbf{A}_{\mathrm{L}}$ is the 24x3 matrix. Differentiating of this spin vector we can get

$$\delta\boldsymbol{\Omega} = \mathbf{A}^{T}_{L}\delta\mathbf{u}_{L} = \mathbf{A}^{T}_{L}\left[diag\,\mathbf{R}^{T}\right]\delta\mathbf{u}_{G} + \mathbf{A}^{T}_{L}\left[col\,(\mathbf{R}^{T}\mathbf{S}(\mathbf{x}^{k1}_{G}))\right]\delta\boldsymbol{\theta} = 0 \tag{26}$$

and

Published By:
Blue Eyes Intelligence Engineering
& Sciences Publication Pvt. Ltd.

$$\delta\boldsymbol{\theta} = -\left[\mathbf{A}_L^T\, col\,(\mathbf{R}^T\mathbf{S}(\mathbf{x}_G^{k1}))\right]^{-1}\mathbf{A}_L^T\left[diag\,\mathbf{R}^T\right]\delta\mathbf{u}_G = \mathbf{V}^T\delta\mathbf{u}_G \quad (27)$$

Consequently using Eq. (24) and Eq. (26)

$$\delta\mathbf{u}_L = \left[diag\,\mathbf{R}^T + col\,(\mathbf{R}^T\mathbf{S}(\mathbf{x}_G^{k1}))\,\mathbf{V}^T\right]\delta\mathbf{u}_G = \mathbf{T}\delta\mathbf{u}_G \quad (28)$$

where $\mathbf{T}$ is the transformation matrix.

E. Tangent Stiffness Matrix

The local internal force vector $\mathbf{F}_{i,L}$ of the 8-node solid-shell element can be determined by

$$\mathbf{F}_{i,L} = \int \mathbf{B}_L^u \boldsymbol{\sigma}_L dV_0 \quad (29)$$

where $\mathbf{B}_L^u$ is the strain-displacement matrix, $\boldsymbol{\sigma}_L$ is the local stress vector. The relationship between the global and local internal force vectors can be given as

$$\mathbf{F}_{i,G} = \mathbf{T}^T\mathbf{F}_{i,L} = \mathbf{T}^T\mathbf{K}_L\mathbf{u}_L \quad (30)$$

where $\mathbf{K}_L$ the linear local stiffness matrix. The global tangent stiffness matrix $\mathbf{K}_T$ can be determined by differentiation of Eq. (30) such as

$$\delta\mathbf{F}_{i,G} = \mathbf{T}^T\delta\mathbf{F}_{i,L} + \delta\mathbf{T}^T\mathbf{F}_{i,L} = (\mathbf{T}^T\mathbf{K}_L\mathbf{T} + \mathbf{K}_{\sigma 1})\delta\mathbf{u}_G = \mathbf{K}_T\delta\mathbf{u}_G \quad (31)$$

where $\mathbf{K}_{\sigma 1}$ is the initial stress matrix. This matrix can be determined using the variation of the transformation matrix $\mathbf{T}$

$$\delta\mathbf{T}^T\mathbf{F}_{i,L} = \delta\left[diag\,\mathbf{R}^T + col\,(\mathbf{R}^T\mathbf{S}(\mathbf{x}_G^{k1}))\,\mathbf{V}^T\right]\mathbf{F}_{i,L} = \mathbf{K}_{\sigma 1}\delta\mathbf{u} \quad (32)$$

If we define a local internal force vector $\tilde{\mathbf{F}}_{i,L}^k$ for a node k such as,

$$\tilde{\mathbf{F}}_{i,L}^k = \mathbf{R}\mathbf{F}_{i,L}^k \quad (33)$$

and then the initial stress matrix $\mathbf{K}_{\sigma 1}$ can take the form of

$$\mathbf{K}_{\sigma 1} = -col\,(\mathbf{S}(\tilde{\mathbf{F}}_{i,L}^k))\mathbf{V}^T + \mathbf{V}row\,(\mathbf{S}(\tilde{\mathbf{F}}_{i,L}^k)) + \mathbf{V}row\,(\mathbf{S}(\mathbf{x}_G^{k1}))\,col\,(\mathbf{S}(\tilde{\mathbf{F}}_{i,L}^k))\mathbf{V}^T \quad (34)$$

however, last term in Eq. (34) produces non-symmetric matrix. The non-symmetric part can be written as

$$\text{Non}-\text{sym} = \frac{1}{2}\sum_{k=1}^{n}(\mathbf{x}_G^{k1}\tilde{\mathbf{F}}_{i,L}^{kT} - \tilde{\mathbf{F}}_{i,L}^k\mathbf{x}_G^{k1T}) \quad (35)$$

Then, the initial stress matrix $\mathbf{K}_{\sigma 1}$ is given by

$$\mathbf{K}_{\sigma 1} = -col\,(\mathbf{S}(\tilde{\mathbf{F}}_{i,L}^k))\mathbf{V}^T + \mathbf{V}row\,(\mathbf{S}(\tilde{\mathbf{F}}_{i,L}^k)) + \mathbf{V}\,\text{sym}\left(\sum_{k=1}^{n}\mathbf{S}(\mathbf{x}_G^{k1})\,\mathbf{S}(\tilde{\mathbf{F}}_{i,L}^k)\right)\mathbf{V}^T \quad (36)$$

As a result, we can write the stiffness matrices used in the incremental-iterative procedure in the matrix form as

$$\mathbf{K}^{uu} = \int_V \bar{\mathbf{B}}_L^{uT}\,\mathbf{D}\,\bar{\mathbf{B}}_L^u\,dV_0 \quad (37)$$

$$\mathbf{K}^{u\alpha} = \int_V \bar{\mathbf{B}}_L^{uT}\,\mathbf{D}\,\bar{\mathbf{B}}_L^\alpha\,dV_0 \quad (38)$$

$$\mathbf{K}^{\alpha\alpha} = \int_V \bar{\mathbf{B}}_L^{\alpha T}\,\mathbf{D}\,\bar{\mathbf{B}}_L^\alpha\,dV_0 \quad (39)$$

where $\mathbf{D}$ is the symmetric 6x6 material matrix.
The enhanced strain parameters $\boldsymbol{\alpha}$ can be eliminated at the element level like follows

$$\delta\boldsymbol{\alpha} = (\mathbf{K}^{\alpha\alpha})^{-1}(\mathbf{K}^{u\alpha T}\,\delta\mathbf{u}_G - \mathbf{F}_{i,L}^\alpha) \quad (40)$$

$$\bar{\mathbf{F}}_{i,L} = \mathbf{F}_{i,L} - \mathbf{K}^{u\alpha}(\mathbf{K}^{\alpha\alpha})^{-1}\mathbf{F}_{i,L}^\alpha \quad (41)$$

$$\mathbf{K}_L = \mathbf{K}^{uu} - \mathbf{K}^{u\alpha}(\mathbf{K}^{\alpha\alpha})^{-1}\mathbf{K}^{u\alpha T} \quad (42)$$

$$\mathbf{K}_T = \mathbf{T}^T\mathbf{K}_L\mathbf{T} + \mathbf{K}_{\sigma 1} \quad (43)$$

where $\mathbf{K}_T$ is the tangent stiffness matrix. And, we can determine the out of balance force $\mathbf{P}$ used in the nonlinear procedure as

$$\mathbf{P} = \mathbf{F}_e - \mathbf{T}^T\bar{\mathbf{F}}_{i,L} \quad (44)$$

where $\mathbf{F}_e$ is the external force.

III. NUMERICAL EXAMPLES

The element stiffness matrix is computed numerically using a 2×2×2 Gauss integration scheme. Most of the results presented here are compared with solutions of Sze. et al. [30] who chosen S4R element in their analysis and SHELL63 element of ANSYS.

A. A Cantilever Subjected To End Shear Force

A cantilever is subjected to an end shear force F, shown in Figure 2. The problem is examined using 20x1 enhanced solid-shell elements. Figure 3 plots the end shear force against the vertical and horizontal tip displacements (called point A) of present, 16x1 S4R and SHELL63 element results. The two solutions are almost the same.

Published By:
Blue Eyes Intelligence Engineering
& Sciences Publication Pvt. Ltd.

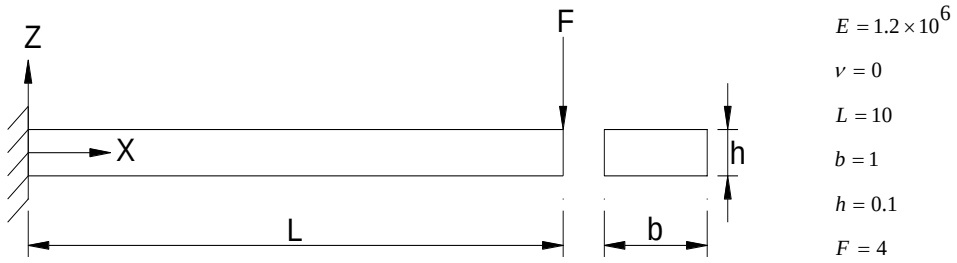

Figure 2. Cantilever Subjected to End Shear Force

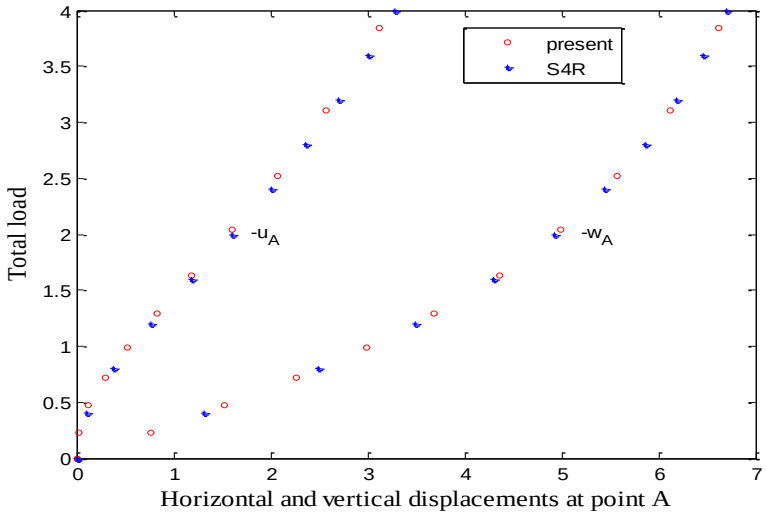

Figure 3. Load–Displacement Curves for Cantilever Subjected to End Shear Force

B. Buckling of A Beam Under Axial Compressive Load

An isotropic beam is subjected to compressive load F, shown in Figure 4. The compressive load is applied with an imperfect angle θ of 0.0573˚ to activate the buckling behavior of the beam. The critical load calculated by the by Euler's formula is $F_{cr} = 1124.21$. Figure 5 plots the compressive force against the vertical and horizontal tip displacements of loaded point (A) and SHELL63 element results are given in the same figure.

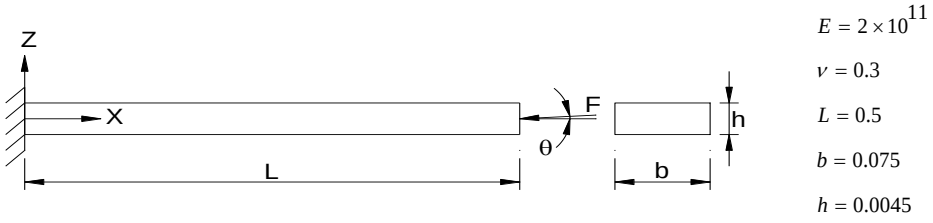

Figure 4. Cantilever Subjected to Compressive Force

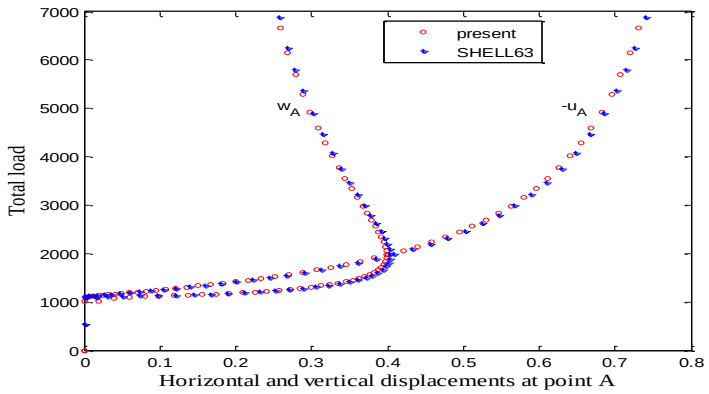

Figure 5. Load–Displacement Curves for the Cantilever Subjected to Compressive Force

C. Hinged Semi-Cylindrical Roof

This is a commonly used benchmark problem for large-displacement analysis of shallow shell subjected to a central pinching force, see Figure 6. The problem was studied many researchers [31-32]. The straight edges are hinged and immovable while the curved edges are free. The structure is modeled with 10x10 enhanced solid-shell elements on one quarter of its surface and with two elements in thickness direction. We investigate the buckling behavior of the cylindrical shell for two different thicknesses. The vertical displacements of loaded point (A) are reproduced in Figure 7 and 8, plotted against the load level and compared to the S4R element solutions. A very good agreement between the solutions along the entire unstable load–displacement path is noticeable.

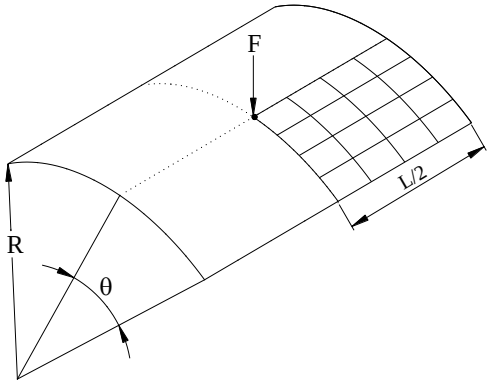

E = 3102.75

ν = 0.3

R = 2540

L = 508

h = 12.7 *or*

h = 6.35

θ = 0.1

Figure 6. Hinged Semi-Cylindrical Roof Subjected to a Central Point Load.

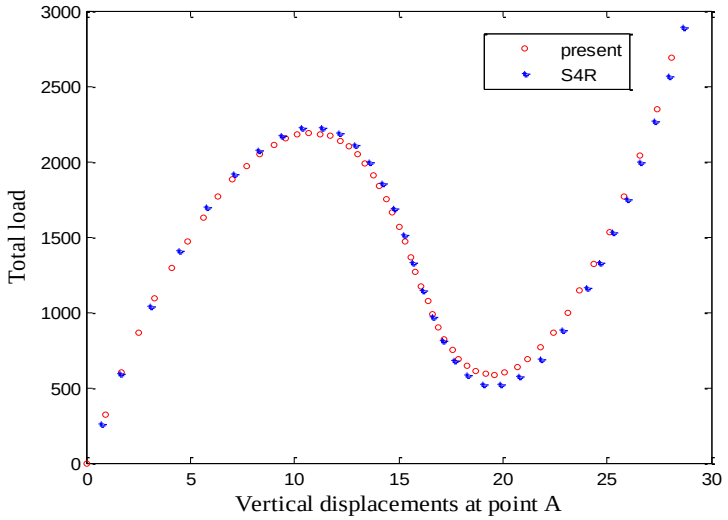

Figure 7. Load–Displacement Curves for the Hinged Semi-Cylindrical Roof for the Thickness h=12.7

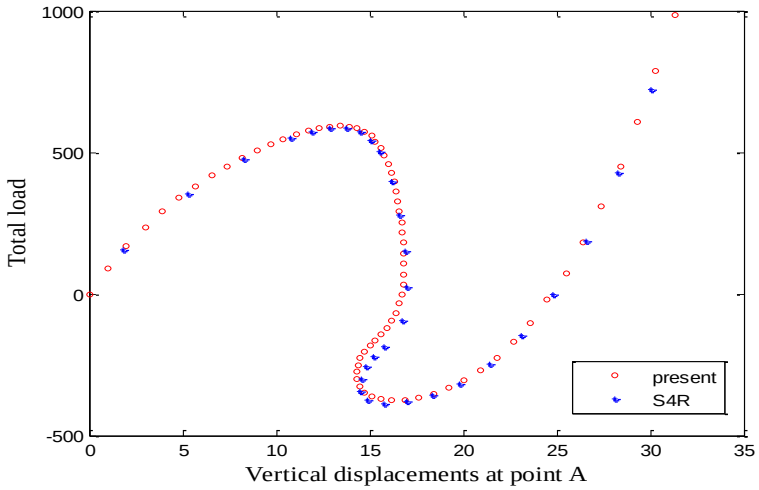

Figure 8. Load–Displacement Curves for The Hinged Semi-Cylindrical Roof for the Thickness h=6.35

D. The Solution Method

If you are using *Word*, use either the Microsoft Equation Editor or the *Math Type* add-on (http://www.mathtype.com) for equations in your paper (Insert | Object | Create New | Microsoft Equation *or* Math Type Equation). "Float over text" should *not* be selected.

IV. CONCLUSION

A nearly locking free formulation of an 8-node solid-shell element based on the co-rotational description of motion was developed. . The enhanced strain method was used to alleviate the locking problems. The polar decomposition theorem was employed to obtain the rotation matrix and the transformation matrix which defines the relationship between the variations of local displacements and furthermore, the variation of the global displacements was also formed. Thus, geometric nonlinearities were taken into account via rotation of the local system. Several benchmark problems were studied to show the reliability of the proposed method.

REFERENCES

1. Polat C., 2010. Co-rotational formulation of a solid-shell element utilizing the ANS and EAS methods, Theoretical and Applied Mechanics, 3(48), 771-788.
2. Polat, C., 2010. An assessment of a co-rotational EAS brick element. Latin American Journal of Solids and Structures. 7, 77–89.
3. Felippa, CA, Haugen, B., 2005. A unified formulation of small strain corotational finite elements: I. Theory. Computer Methods in Applied Mechanics and Engineering 194, 2285-2335.
4. Wempner, G., 1969. Finite elements, finite rotations and small strains of flexible shells. The International Journal of Solids and Structures 5, 117-153.
5. Argyris, JH., Bahner, H., Doltsnis, J., et al. 1979. Finite element method-the natural approach. Computer Methods in Applied Mechanics and Engineering 17/18, l-106.
6. Belytschko, T., Glaum, LW., 1979. Application of higher order corotational stretch theories to nonlinear finite element analysis. Computers and Structures 10, 175-182.
7. Crisfield, MA., Moita, GF., 1996. A co-rotational formulation for 2-D continua including incompatible modes. International Journal of Numerical Methods in Engineering 39, 2619-2633.
8. Moita, GF., Crisfield, MA., 1996. A finite element formulation for 3-d continua using the co-rotational technique. International Journal of Numerical Methods in Engineering 39, 3775-3792.
9. Urthaler, Y., Reddy, JN., 2005. A corotational finite element formulation for the analysis of planar beams. Communications in Numerical Methods in Engineering 21, 553-570.
10. Hauptmann, R., Schweizerhof, K., 1998. A systematic development of 'solid-shell' element formulations for linear and non-linear analyses employing only displacement degrees of freedom. International Journal for Numerical Methods in Engineering 42, 49-69.
11. Miehe, C., 1998. Theoretical and computational model for isotropic elastoplastic stress analysis in shells at large strains. Computer Methods in Applied Mechanics and Engineering 155, 193-233.
12. Hauptmann, R., Scheizerhof, K., Doll, S., 2000. Extension of the "solid-shell" concept for application to large elastic and large elastoplastic deformations. International Journal for Numerical Methods in Engineering 49, 1121-1141.
13. Sze, KY., Yao, LQ., 2000. A hybrid stress ANS solid-shell element and its generalization for smart structure modelling. Part I: solid-shell element formulation. International Journal of Numerical Methods in Engineering 48, 545-564.
14. Sze, KY., Yao, LQ., Yi, S., 2000. A hybrid stress ANS solid-shell element and its generalization for smart structure modelling. Part II: smart structure modelling. International Journal of Numerical Methods in Engineering 48, 565-582.
15. Harnau, M., Schweizerhof, K., 2002. About linear and quadratic "solid-shell" elements at large deformations. Computers and Structures 80, 805-817.
16. Vu-Quoc, L., Tan, XG., 2003. Optimal solid shells for non-linear analyses of multilayer composites. I. Statics. Computer Methods in Applied Mechanics and Engineering 192, 975-1016.
17. Sousa, RJA., Cardoso, RPR., Fontes Valente, RA., Yoon, YW., Gracio, JJ., Natal Jorge, RM., 2004. A new one-point quadrature enhanced assumed strain (eas) solid-shell element with multiple integration points along thickness- part 1: geometrically linear applications. International Journal for Numerical Methods in Engineering 62, 952-977.
18. Tan, XG., Vu-Quoc, L., 2005. Optimal solid shell element for large deformable composite structures with piezoelectric layers and active vibration control. International Journal of Numerical Methods in Engineering 64, 1981-2013.
19. Sousa, RJA., Cardoso, RPR., Valente, RAF., Yoon, JW., Gracio, JJ., Jorge, RMN., 2006. A new one-point quadrature Enhanced Assumed Strain solid-shell element with multiple integration points along thickness Part II – Nonlinear Applications, International Journal of Numerical Methods in Engineering 67, 160-188.
20. Zienkiewicz, OC., Taylor, RL., Too, JM., 1971. Reduced integration techniques in finite element method. International Journal for Numerical Methods in Engineering 3, 275-290.
21. Hughes, TJR., Taylor, RL., Kanoknukulchai, W., 1977. A simple and efficient finite element for plate bending. International Journal for Numerical Methods in Engineering 11, 1529-1543.
22. Hughes, TJR., Cohen, M., Haroun, M., 1978. Reduced and selective integration techniques in the finite element analysis of plates. Nuclear Engineering and Design 46, 203-222.
23. Bathe, KJ., Dvorkin, EN., 1986. A formulation of general shell elements- The use of mixed interpolation of tensorial components. International Journal for Numerical Methods in Engineering 22, 697-722.
24. Bucalem, ML., Bathe, KJ., 1993. Higher-order MITC general shell elements. International Journal for Numerical Methods in Engineering 36, 3729-3754.
25. Simo, JC., Rifai, MS., 1990. A class of mixed assumed strain methods and the method of incompatible modes. International Journal for Numerical Methods in Engineering 29, 1595-1638.
26. Andelfinger, U., Ramm, E., 1993. EAS-elements for two-dimensional, three-dimensional, plate and shell structures and their equivalence to HR-elements. International Journal for Numerical Methods in Engineering 36, 1311-1337.
27. Klinkel S., Wagner W., 1997. A geometrical non-linear brick element. International Journal for Numerical Methods in Engineering 40, 4529-4545.
28. Valente, RAF., 2004. Developments on shell and solid-shell finite elements technology in nonlinear continuum mechanics. Ph.D. Thesis, University of Porto, Portugal.
29. Alves de Sousa RJ, Natal Jorge RM, Fontes Valente RA, César Sá JMA., 2003. A new volumetric and shear locking-free EAS element. Engineering Computations, 20, 896–925.
30. Sze, KY., Liu, XH., Lo, SH., 2004. Popular benchmark problems for geometric nonlinear analysis of shells. Finite Elements in Analysis and Design 40, 1551-1569.
31. Kreja I., Schmidt R., Reddy, JN., 1997. Finite elements based on a first-order shear deformation moderate rotation shell theory with applications to the analysis of composite structures, International Journal of Non-Linear Mechanics 32, 1123–1142.
32. Chróścielewski J., Makowski J., Stumpf H., 1992. Genuinely resultant shell finite elements accounting for geometric and material non-linearity, International Journal for Numerical Methods in Engineering 35, 63–94.